Feedback control of the vortex-shedding instability based on sensitivity analysis

Simone Camarri, Angelo Iollo

Feedback control of the vortex-shedding instability based on sensitivity analysis

Simone Camarri[1,a)] and Angelo Iollo[2]
[1]*Dipartimento di Ingegneria Aerospaziale, Università di Pisa, via G. Caruso 8, 56122 Pisa, Italy*
[2]*Institut de Mathématiques de Bordeaux UMR 5251 CNRS, Université Bordeaux 1 and INRIA Bordeaux—Sud Ouest, Equipe-Projet MC2, 351 Cours de la Libération, 33405 Talence Cedex, France*

(Received 23 February 2010; accepted 14 July 2010; published online 14 September 2010)

In the present work, a simple proportional feedback control is designed to suppress the vortex-shedding instability in the wake of a prototype bluff-body flow, i.e., the flow around a square cylinder confined in a channel with an incoming Poiseuille flow. Actuation is provided by two jets localized on the cylinder surface and velocity sensors are used for feedback control. This particular configuration is a pretext to propose a more general strategy for designing a controller, which is independent of the type of actuation and sensors. The method is based on the linear stability analysis of the flow, carried out on the unstable steady solution of the equations, which is also the target flow of the control. The idea is to use sensitivity analysis to predict the displacement in the complex plane of some selected eigenvalues, found by the linear stability analysis of the flow, as a function of the control design parameters. In this paper, it is shown that the information provided by only sensitivity analysis carried out on the uncontrolled system is not sufficient to design a controller which stabilizes the flow. Therefore, the control is designed iteratively by successive linearizations. Apart from possible constraints, the position of the sensors, the direction along which velocity is measured, and the feedback coefficients are outputs of the design procedure. The proposed strategy leads to a successful control up to a Reynolds number which is at least twice as large as the critical one for the primary instability, using only one velocity sensor. © *2010 American Institute of Physics*. [doi:10.1063/1.3481148]

I. INTRODUCTION

When the Reynolds number exceeds a critical value, alternate vortex-shedding occurs in the wake of bluff-bodies, causing an increase in mean drag, oscillating lift, and related effects (vibrations, noise, resonance, etc.). Therefore, the control of vortex-shedding is central in many engineering applications and a large number of works in the literature are dedicated to this problem, as documented in the recent review by Choi *et al.*[1] The methods to control vortex-shedding can be divided in passive (no power required), active open-loop (no sensors required), and active closed-loop controls. Especially in the past, many passive controls have been proposed due to the simplicity in their practical implementation. Although passive controls do not need energy, they must be designed for a precise flow condition, and off-design performance can be poor. Conversely, open-loop active controls have margin to adapt to different flow conditions; however, they need a continuous energy supply. In order to obtain controls that are even more closely linked to the actual flow conditions and energetically more efficient (in the sense that they can stabilize the steady solution with zero actuation), closed-loop strategies are necessary.

Among closed-loop controls, an important class is given by the linear feedback controls, since they can be easily implemented in real applications. Several examples of this kind of control are documented in the literature. For instance, Roussopoulos[2] carried out experiments in controlling the wake of a circular cylinder using a single-sensor and a loudspeaker for actuation, and he was able to increase the flow critical Reynolds number for the onset of vortex-shedding by a factor of about 20%. Also Huang[3] used a loudspeaker as an actuator, measuring the velocity near one of the two shear layers. In his simulations of the flow around a circular cylinder, Park *et al.*[4] used a proportional feedback between a velocity sensor, placed on the symmetry line of the flow, and a synchronized pair of blowing/suction slots on the cylinder surface. They showed that the success of the control was dependent on the sensor position and they were able to stabilize the flow up to $\mathrm{Re} \simeq 60$ ($\mathrm{Re}_{cr} \simeq 47$ for this flow). Above this limit, other modes were destabilized by the controller, showing an important feature of the considered flow: although only a pair of complex-conjugate unstable modes can be identified by a linear stability analysis, there are other modes which can be strongly affected and possibly destabilized by the controller, leading to the well-known "waterbed effect." This aspect is discussed in detail by Roussopoulos,[2] too, where it is experimentally shown that increasing the feedback gain outside the range of values leading to a stable wake, other modes become unstable. It is also shown that the range of feedback gains leading to stability shrinks as the Reynolds number of the flow is increased. Zhang *et al.*[5] proposed different proportional-integral-derivative (PID) controllers to suppress the vortex-shedding and the resonant in-

a)Electronic mail: s.camarri@ing.unipi.it.

duced vibrations in the flow around a square cylinder mounted on an elastic support. Experimental tests were carried out, in which actuation was provided by three piezoelectric ceramic actuators positioned on the cylinder surface. Two sensors were used, one measuring the velocity signal in the wake by a hot-wire probe and the other the displacement of the cylinder. The coefficients of the controller were set heuristically. They showed that the proportional part of the PID controller is the most effective one in the control of the vortex-shedding, as it causes a change in the system damping. Moreover, if only one sensor is used, measuring the velocity in the wake is definitely more effective than measuring the cylinder displacement, even if the best results were obtained with a combined use of both the signals. In that case, the vortex-shedding was significantly damped at Re=3500.

In the literature there are also several examples of application of optimal control theory for the control of vortex-shedding. In this case, two major aspects for the success of the control are (1) the choice of the objective function that the control should minimize and (2) the choice of the temporal window for the optimization. While a few shedding cycles seem to be sufficient for point (2), point (1) is very critical. Moreover, due to the complexity of the problem, it is not assured that a global minimum of the objective function is found in the iterative design of the controller. Lastly, in this kind of controls, it is often assumed that the full-state of the flow field is available for a global time period, an assumption that, together with the computational costs associated with this control strategy due to the number of degrees of freedom involved in the flow simulation, makes a direct implementation of this control strategy not possible in practice without the use of an approximate flow observer and/or a simplified flow model. On the other hand, it has been proven that complete stabilization of the incompressible Navier–Stokes equations via wall-actuation is possible when using full-state feedback (Raymond[6]), but when a limited number of sensors is used, this property no longer holds. Numerical examples in this direction are given, for instance, by He *et al.*[7] and Protas and Styczek.[8] Note that in the two examples cited above, although actuation is strong (cylinder rotation), the vortex-shedding was never completely suppressed.

Some of the difficulties of the optimal control are bypassed by relaxing the optimality condition of the controller, as done, for instance, in the suboptimal control strategy, applied, for example, for the suppression of the vortex-shedding in the wake of a circular cylinder by Min and Choi.[9] In this case actuation is provided by blowing/suction on the cylinder surface, on which distributed pressure sensors are used. When a realistic portion of the surface is used both for sensing and actuating (ratio of 1:8 with respect to the total surface), the vortex-shedding is damped but not suppressed at Re=100; conversely, when all the cylinder surface is used, the flow is stabilized up to Re=160. This example illustrates the important role played by distributed actuators and sensors for the success of the control and highlights the difficulty of obtaining a successful control with limited and realistic actuation/sensors.

The computational costs associated with the manipulation of the flow model, as it involves a very large number of degrees of freedom which also increases with the flow Reynolds number, are major problem for the design of the controller, whatever control strategy is adopted. This limit is partially bypassed by the use of reduced-order models (ROMs) for the flow. The basic idea is to design the control on the ROM and then apply it to the complete system. The major problem of this approach is the accuracy of the ROM in representing the true actuated flow. Often the ROM is based on proper orthogonal decomposition (POD). Examples of POD-based optimal controls are given by Graham *et al.*,[10] Bergmann *et al.*,[11] and by Siegel *et al.*[12] for the circular cylinder and by Weller *et al.*[13] for a confined square cylinder. ROMs can also be based on strategies different from POD, as in Li and Aubry[14] (Re=100 and Re=200) or in Protas[15] (Re=75). Another example in this direction is given by Pastoor *et al.*,[16] in which the ROM is based on a physics-inspired vortex model, the flow around a D-shaped body is considered and the control allows a 15% reduction of the drag with a zero-net-mass-flux actuation in experiments of the flow up to $\mathrm{Re}=7\times10^4$. Reduced-order models are often used to build flow observers, too, which are a necessary ingredient for those control strategies that need the whole flow field to be available at each instant in time. Such models for a flow observer also suggest strategies for optimal sensor placement. Examples in this direction are given, for instance, by Mokhasi and Rempfer,[17] Cohen *et al.*,[18] Willcox,[19] and Buffoni *et al.*[20] In the work by Antoniades and Christofides,[21] the sensor placement is optimized together with the controller design for a one-dimensional quasilinear parabolic partial-differential equation modeling a reaction-diffusion phenomenon.

A recent and attractive prospective for vortex-shedding control is given by control design based on the results obtained by the global stability and sensitivity analysis of the primary instability of the wake. The spirit of this approach, as depicted in Ref. 1, is to modify the flow so as to stabilize or, in general, affect the characteristics of its global instability, which is here the primary instability of the wake. The modifications can be obtained, for instance, by introducing a passive or open-loop control. To this purpose, Giannetti and Luchini[22] carried out a linear sensitivity of the primary instability to a localized volume reaction force and the resulting sensitivity maps were used to localize the wavemaker of the global instability. In Marquet *et al.*[23] a similar analysis was carried out, but the effect of the baseflow modifications on the instability caused by the application of a localized volume reaction force was taken into account too. As a result, maps were provided which show the sensitivity of the primary instability to a localized action on the flow, such as the introduction of a very small cylinder.

The control strategy that we propose in the present work is closely related to the passive control design inspired by the results coming from the global and sensitivity analysis of the primary instability described above. In particular, in that case, the baseflow is modified for controlling the instability. At difference, in our case the baseflow is unchanged, and the properties of the global instability are changed by varying

the structure of the linearized equations subsequent to the introduction of an active feedback control of the flow. For this reason, the analysis which is at the base of the present work is the one documented by Giannetti and Luchini.[22] The strategy proposed here for the design of the control is the following: we consider a feedback control with actuators fixed *a priori*, this will be characterized by a set of free parameters. A sensitivity analysis of a prescribed set of eigenvalues, associated with selected global modes, is carried out with respect to the design parameters. In particular, the selected modes are the unstable ones and those which might be destabilized by the adopted actuation. Afterwards, the control parameters are varied by successive linearizations and sensitivity analyses in order to move the monitored eigenvalues in a specified region of the complex plane, which will be contained in the stable half of the complex plane if the objective of the control is the stabilization of the steady solution of the equations. Since the control that we propose does not alter the steady solution, the sensitivity analysis only involves the linearized equations, as in Giannetti and Luchini.[22] If the baseflow is modified, for instance if we want to mimic in the flow real sensors with a given size, the analysis documented by Marquet *et al.*[23] should be used instead. Thus, the main objective of the present work is to propose a strategy to utilize the information content provided by the sensitivity analysis of the primary instability to design a control for its suppression. In this paper we develop the main ideas of our design strategy by considering a particular and simple control, which might be easily implemented in an experiment: a proportional feedback control based on velocity sensors which drive two blowing/suction jets on the cylinder surface, with a realistic size and mass rate. As a prototype of bluff-body flow, we consider the flow around a square cylinder which is confined within a channel with a low blockage ratio ($L/H=1/8$, L being the length of the cylinder edges and H the channel height, respectively) with an incoming Poiseuille flow (for the characteristics of this flow see, for instance, Camarri and Giannetti,[24] Turki *et al.*,[25] and Breuer *et al.*[26]). This particular flow configuration does not affect the generality of the approach presented. The actuation is fixed *a priori* in this work, and it is identical to that used by Weller *et al.*[13] In that work, an optimization strategy is proposed to minimize the unsteadiness of the vortex-shedding phenomenon by a proportional feedback control. The feedback is designed by using a nonlinear method based on a POD reduced-order model. As already stated, a similar actuation, driven in feedback by one velocity sensor, is used by Park[4] and by Min and Choi[9] for the case of a circular cylinder in unconfined flow.

In the present case, the design parameters of the controller are the position of the sensors, the direction along which the velocity is measured, and the associated feedback coefficients. The sensitivity analysis of the primary instability with respect to those design parameters provides (a) a physically based criterion for the initial placement of the sensors and (b) an efficient way to evaluate the linearized displacement in the complex plane of the unstable eigenvalue associated with the vortex-shedding instability as a function of the control parameters. Since the analysis described above is linearized, it is generally accurate only for a small variation of the parameters. However, especially at Reynolds numbers well above the critical one for flow stability, the unstable eigenvalues need to be significantly displaced in the complex plane to make the system linearly stable. This implies that the stabilizing control represents a perturbation of the system that goes beyond the validity limits of the linearized analysis carried out on the uncontrolled state. Therefore, the overall design of the controller is carried out iteratively by successive linearizations, i.e., the results of a sensitivity analysis are used to modify the controller parameters within the validity limits of the linearized analysis itself, and, to progress further in the design of the controller, a new linearization and a new sensitivity analysis are carried out. This process continues until the unstable eigenvalues to be controlled reach a prescribed region in the complex plane. As also stressed by Park *et al.*,[4] it may happen that, while trying to stabilize an unstable eigenvalue, other stable modes might be negatively affected by the controller and eventually become unstable. In order to avoid this situation, potentially dangerous but stable eigenvalues of the linearized system are also taken into account in the design of the controller, and, for this purpose, their displacement is predicted by the same sensitivity analysis mentioned above. In a sense the present method mimics a partial pole-placement of the system, which involves the unstable and the monitored eigenvalues. In this case, however, a pole-placement would be extremely expensive (if not practically impossible) due to the size of the discrete system to be controlled [for instance, in the present two-dimensional (2D) simulations, the number of degrees of freedom approximately varies between 5.0×10^5 and 1.2×10^6!].

II. STATEMENT OF THE PROBLEM

We consider the problem of designing a proportional feedback control whose target is the stabilization of the vortex-shedding instability developing in an incompressible flow past a cylinder. In particular, at a supercritical Reynolds number for vortex-shedding instability, the controller is required to suppress the unsteadiness and hence to stabilize the steady unstable solution of the flow equations (target flow).

The actuators are two blowing/suction jets on the cylinder surface, with a realistic size and mass rate. The number of actuators and their type is not limited *a priori*. However, the position of the jets is fixed here, for a comparison with other control strategies documented in the literature. The two jets are driven by only one signal and they are 180° out of phase, so that the global mass flux is instantaneously null.

A minimal number of velocity sensors is used for the feedback. The proposed strategy provides information on where to place the sensors and allows the optimization of their position and the progressive enrichment of their number during the design process. The component of the velocity which is measured by the sensor can be left as an unconstrained parameter and subsequently optimized.

If the controller is successfully designed, it is at least certain that the flow is controlled as long as the controller is activated when the flow is sufficiently close to the target flow, since its design is based on the Navier–Stokes equa-

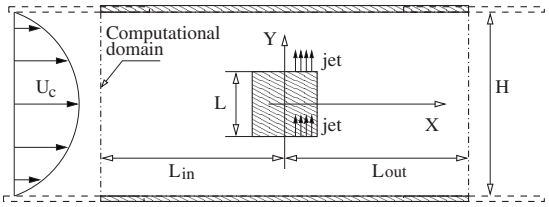

FIG. 1. Flow configuration, frame of reference and computational domain (not in scale).

tions linearized on the target flow. In this case, indeed, the target flow is a (linearly) stable fixed point of the controlled flow but no information is provided on its basin of attraction, which thus can only be explored *a posteriori*, as for all controls based on the linearized dynamics of the system to be controlled.

III. FLOW CONFIGURATION, GOVERNING EQUATIONS, AND NUMERICAL TOOLS

The incompressible flow around an infinitely long square cylinder, symmetrically confined by two parallel plates with an incoming Poiseuille flow, is considered here. With reference to Fig. 1, the blockage ratio is $\beta=L/H=1/8$ and the Reynolds number is defined as $\mathrm{Re}=U_cL/\nu$, ν being the kinematic viscosity of the fluid. If not explicitly specified, the quantities reported in this work are made nondimensional using L and U_c as the reference length and velocity, respectively. The Reynolds numbers considered in the present work are such that the flow is expected to be independent of the spanwise (z) direction. The flow is thus described by the two-dimensional Navier–Stokes equations which, once normalized using U_c and L, can be written as follows:

$$\frac{\partial \mathbf{U}}{\partial t} + \mathbf{U}\cdot\nabla\mathbf{U} = -\nabla P + \frac{1}{\mathrm{Re}}\Delta\mathbf{U}, \tag{1}$$

$$\nabla\cdot\mathbf{U} = 0, \tag{2}$$

where $\mathbf{U}$ is the velocity vector and P the reduced pressure. Furthermore, no-slip conditions are imposed on the confining walls, the Pouiseuille velocity profile is enforced at the inflow boundary, and convective boundary conditions are applied at the outflow boundary. As to the cylinder surface, this is divided into two parts, one (S_j) with jets and one (S_w) without. No-slip boundary conditions are imposed on S_w, while a constant velocity profile is imposed on S_j, with the velocity oriented in the direction normal to the cylinder surface ($\mathbf{U}=U\mathbf{n}$). Note that a different velocity profile at the jet exit, as well as the position of the jets on the cylinder surface, might influence the effectiveness of the actuation. However, the strategy for designing the controller described in what follows would remain the same. The jet intensity U is given by a feedback controller, using N_s velocity sensors placed at points (x_s,y_s) that feed the velocity measured in the direction $\mathbf{d}_s$ back to the jet through a coefficient K_s,

$$U(x,y,t) = \sum_{s=1}^{N_s} K_s[\mathbf{U}(x_s,y_s,t) - \mathbf{U}_b(x_s,y_s,t)]\cdot\mathbf{d}_s, \quad (x,y)\in S_j, \tag{3}$$

where $\mathbf{U}_b$ is the reference velocity field corresponding to the steady solution of the Navier–Stokes equations in this case. Feedback (3) guarantees that $Q_b=(\mathbf{U}_b,P_b)$ is a steady solution both with and without control. In the 2D linear stability analysis of the solution Q_b, a small amplitude disturbance is considered, having the following form:

$$\mathbf{u}(x,y,t) = \hat{\mathbf{u}}(x,y)\exp(\sigma t), \tag{4}$$

$$p(x,y,t) = \hat{p}(x,y)\exp(\sigma t). \tag{5}$$

The equations governing the evolution of the disturbance, once linearized, become

$$\sigma\hat{\mathbf{u}} + \mathbf{U}_b\cdot\nabla\hat{\mathbf{u}} + \hat{\mathbf{u}}\cdot\nabla\mathbf{U}_b - \frac{1}{\mathrm{Re}}\Delta\hat{\mathbf{u}} + \nabla\hat{p} = 0, \tag{6}$$

$$\nabla\cdot\hat{\mathbf{u}} = 0 \tag{7}$$

along with homogeneous boundary conditions on S_w and with the following condition on S_j:

$$\mathbf{u}(x,y,t) = \left[\sum_{s=1}^{N_s} K_s\mathbf{u}(x_s,y_s,t)\cdot\mathbf{d}_s\right]\mathbf{n}, \quad (x,y)\in S_j. \tag{8}$$

According to the boundary conditions imposed on $\mathbf{U}$ and $\mathbf{U}_b$, the disturbance velocity $\mathbf{u}$ vanishes on the confining walls and at the inflow boundary, while convective boundary conditions are imposed at the outflow. The resulting problem is a generalized eigenvalue problem and the flow is stable, provided that all the eigenvalues σ of the problem are such that $\mathrm{Re}(\sigma)<0$.

In the present work, the Navier–Stokes equations and its linearized version have been discretized in space, in conservative form, by a standard staggered, centered finite-difference scheme which is accurate to second-order. An immersed-boundary technique which preserves second-order spatial accuracy is used to satisfy the boundary conditions on the cylinder surface (see Giannetti and Luchini,[22] for details). The steady solution (Q_b) of the equations has been found using a Newton–Raphson method, and the linear system resulting at each iteration is solved by a sparse LU factorization.[27] A subset of the spectrum of the discrete generalized eigenvalue problem resulting from the discretization of Eqs. (6) and (7) has been computed using the Krylov–Schur method implemented in the "slepc" library.[28] For a first localization of the eigenvalues, we estimated part of the spectrum of the linear operator obtained by advancing Eqs. (6) and (7) in time using an implicit Euler scheme. The eigenvalues so obtained have been used as points in the complex plane for a shift-and-invert spectral transformation of the problem, which allowed a successive refinement in the estimation of the eigenvalues (see Ref. 28, for details).

The unsteady Navier–Stokes equations have also been integrated in time to check the behavior of the identified control laws. In this case, we used a standard Adams–

Bashfort/Crank–Nicholson scheme, in which the diffusive terms and the pressure field are treated implicitly and the convective terms explicitly.

The numerical tools used in this work and described above have already been validated for the particular flow considered here, as documented by Camarri and Giannetti.[24]

IV. ALGORITHM FOR DESIGNING THE FEEDBACK CONTROL

A. Sensitivity of a global mode to the feedback action

Once discretized, Eqs. (6) and (7), together with the associated boundary conditions, can be written in the following form:

$$\mathbf{A}\cdot\mathbf{W}=\left[\mathbf{A}_0(\mathrm{Re})+\sum_{s=1}^{N_s}K_s\mathbf{C}(x_s,y_s,\theta_s)\right]\cdot\mathbf{W}=\sigma\mathbf{B}\cdot\mathbf{W}, \tag{9}$$

in which $\mathbf{W}$ is the discrete vector of the unknowns (disturbance velocity and pressure on the grid nodes), θ_s is the angle between the x-axis and the measured component of velocity at the point (x_s,y_s) ($\mathbf{d}_s=(\cos(\theta_s),\sin(\theta_s))$), $\mathbf{A}_0$, $\mathbf{C}$, and $\mathbf{B}$ are the real-valued matrix functions associated with the discretized system, and they implicitly and obviously depend also on the spatial discretization (number and position of the grid nodes). Note that matrix $\mathbf{A}$, due to the feedback control to be summed to the uncontrolled system $\mathbf{A}_0$, also depends on the position of the actuators and on the velocity profile which is assumed at the exit of the jets. However, since we are assuming here that actuation is assigned *a priori*, we have not explicitly highlighted this dependence in Eq. (9).

Suppose that a particular eigenvalue of system (9) is found, σ_k (with the associated eigenvector $\mathbf{W}_k$), and we want to evaluate the variation of its position in the complex plane as the parameters of the control system are varied. We recall that the parameters of the control system are (i) the feedback coefficients, (ii) the position of the sensors, and (iii) the direction of the velocity that is measured by each sensor. Using $\delta\mathbf{A}$ to denote the variation of the system matrix $\mathbf{A}$ of the controlled flow due to the variation of the control parameters, the problem becomes the estimation of the variation of the eigenvalue $\delta\sigma_k$ caused by $\delta\mathbf{A}$. A standard linear analysis leads to the following result:

$$\delta\sigma_k=\frac{\langle\boldsymbol{\xi}_k,\delta\mathbf{A}\cdot\mathbf{W}_k\rangle}{\langle\boldsymbol{\xi}_k,\mathbf{B}\cdot\mathbf{W}_k\rangle}, \tag{10}$$

where $\langle\mathbf{a},\mathbf{b}\rangle=\mathbf{a}^*\cdot\mathbf{b}$ is the scalar product between two complex vectors $\mathbf{a}$ and $\mathbf{b}$ (the asterisk stands for complex-conjugate) and $\boldsymbol{\xi}_k$ is the eigenvector associated with the following system:

$$\mathbf{A}^*\boldsymbol{\xi}_k=\sigma_k^*\mathbf{B}^*\boldsymbol{\xi}_k. \tag{11}$$

As regards the dependence of matrix $\mathbf{C}$ with respect to θ_s, we have

$$\mathbf{C}(x_s,y_s,\theta_s)=\mathbf{C}(x_s,y_s,0)\cos(\theta_s)+\mathbf{C}(x_s,y_s,\pi/2)\sin(\theta_s). \tag{12}$$

Consequently, the variation of the system matrix $\delta\mathbf{A}$ resulting from the variation of the control parameters can be written as follows:

$$\begin{aligned}\delta\mathbf{A}=\sum_{s=1}^{N_s}\Bigg\{&\mathbf{C}(x_s,y_s,\theta_s)\,\delta K_s+\left[K_s\frac{\partial\mathbf{C}}{\partial x_s}(x_s,y_s,\theta_s)\right]\delta x_s\\&+\left[K_s\frac{\partial\mathbf{C}}{\partial y_s}(x_s,y_s,\theta_s)\right]\delta y_s\\&+K_s[\mathbf{C}(x_s,y_s,\pi/2)\cos(\theta_s)-\mathbf{C}(x_s,y_s,0)\sin(\theta_s)]\delta\theta_s\Bigg\}.\end{aligned} \tag{13}$$

When Eq. (13) is substituted in Eq. (10), the variation of the eigenvalue $\delta\sigma_k$ is directly related to the variation of the control parameters by means of a linearized analysis.

B. Design of the controller

In the present work, we use information provided by Eq. (13) to displace some eigenvalues in the complex plane in order to stabilize the flow. There are many ways to achieve this objective. We now describe the strategy followed in the present work. Let us define a generic real function f which depends on the position of N_a selected eigenvalues in the complex plane: $f(\sigma_1,\sigma_2,\ldots,\sigma_{N_a})$. This function is designed so that it reaches a minimum when the considered eigenvalues lie in a particular region of the complex plane, which is chosen *a priori* to stabilize the flow and, if possible, to guarantee particular characteristics to the controlled system. As an example, we could define a function depending on the unstable eigenvalues and let this function assume a minimum value as soon as the eigenvalues enter into the stable region of the complex plane.

The function f is, indirectly, a function of the control parameters, since they obviously affect the position of the eigenvalues of the system. Consequently, the design of the controller will be carried out by minimizing the function f with respect to the control parameters. In this process, information provided by Eq. (13) is used to evaluate the variations of f with respect to the control parameters,

$$\begin{aligned}\delta f(\sigma_1,\sigma_2,\ldots,\sigma_{N_a})&=\sum_{k=1}^{N_a}\left[\frac{\partial f}{\partial\,\mathrm{Re}(\sigma_k)}(\sigma_1,\sigma_2,\ldots,\sigma_{N_a})\,\delta\,\mathrm{Re}(\sigma_k)\right.\\&\left.+\frac{\partial f}{\partial\,\mathrm{Im}(\sigma_k)}(\sigma_1,\sigma_2,\ldots,\sigma_{N_a})\,\delta\,\mathrm{Im}(\sigma_k)\right],\end{aligned} \tag{14}$$

where $\delta\sigma_k$ resulting from variations of the control parameters are given by Eq. (10) and Re() and Im() stand for real and imaginary part of a complex number, respectively. We may note here that the choice of f is arbitrary and depends both on the properties of the target control and on the particular

numerical scheme used to minimize f. Indeed, depending on the numerical method used to minimize f, particular properties of f might be important (for instance, to accelerate convergence). Note also that, since the feedback coefficients are real, the resulting matrix of the controlled system is real-valued and, thus, eigenvalues are real or couples of complex-conjugate numbers; for this reason, it is sufficient to monitor only the eigenvalues with a non-negative imaginary part, keeping only those eigenvalues as arguments of f for the design of the controller. In the present work, f is defined as follows:

$$f(\sigma_1,\sigma_2,\ldots,\sigma_{N_a}) = \sum_{k=1}^{N_a} f_b(\mathrm{Re}(\sigma_k), r_t), \tag{15}$$

where

$$f_b(r,r_t) = \begin{cases} 10\dfrac{(r-r_t)^4}{r_t^4} & \text{if } r_t \le r, \\ 0 & \text{otherwise.} \end{cases} \tag{16}$$

Consequently, the minimum value of f, which is equal to 0, is reached when the real part of all the N_a controlled eigenvalues is negative (stable eigenvalues) and smaller than the target value $r_t<0$, which is thus the stability margin required for the eigenvalues. If the minimum value of f is reached, then the N_a controlled eigenvalues are in the stable region of the complex plane, but other eigenvalues might have become unstable due to the action of the feedback control. For this reason, at the end of each successful minimization of f, it is necessary to check again the whole spectrum of the controlled problem to be sure that the controlled state is linearly stable. However, if the most dangerous eigenvalues of the system are identified and monitored through the function f, there are good chances that the minimization of f will lead to a stable controlled system.

In principle, if no particular constraint is imposed on the position and type of velocity sensors used, then there are four scalar control parameters for each sensor, i.e., its position $((x_s,y_s))$, the direction of measured velocity (θ_s), and the associated feedback coefficient (K_s). Obviously, there is a high degree of freedom on how to start the design of the controller (initial position of the sensors, number of sensors, etc.). Moreover, it is possible to add sensors during the design of the control if, for instance, the final position of the eigenvalues in the controlled system is not satisfactory. When a new sensor is added, the same criteria used for the initial placement of the sensors can be used.

C. Initial position of the sensors

Let us suppose that one sensor needs to be added to the system whose associated matrix is A (A_0 if the sensor is added to the uncontrolled system). According to Eqs. (10) and (13), the variation of a generic eigenvalue σ_k caused by an infinitesimal gain δK_s is

$$\delta\sigma_k = \delta K_s m_k(x_s,y_s,\theta_s), \tag{17}$$

where $m_k(x_s,y_s,\theta_s)$ is given by

$$m_k(x_s,y_s,\theta_s) = \frac{\langle \boldsymbol{\xi}_k, \mathbf{C}(x_s,y_s,\theta_s)\cdot\mathbf{W}_k\rangle}{\langle \boldsymbol{\xi}_k, \mathbf{B}\cdot\mathbf{W}_k\rangle}. \tag{18}$$

The function $m_k(x_s,y_s,\theta_s)$ is a complex-valued function of space and its value on a generic point (x_s,y_s) represents the sensitivity of σ_k to the introduction of a sensor in that point, measuring the velocity in the direction given by θ_s, and feeding its output to the actuators by an infinitesimal feedback coefficient δK_s. In this sense, the function $m_k(x_s,y_s,\theta_s)$ is a sensitivity map of σ_k with respect to the position of the sensor and to the component of measured velocity. In order to understand the structure of the matrix $\mathbf{C}$ and, consequently, of the sensitivity map m_k, let us suppose for the moment that the sensor can be placed only discretely on the nodes of the grid, and that it measures only the horizontal component of velocity ($\theta_s=0$). In this case it is easy to show that the matrix $\mathbf{C}$ is made up of only one column, whose elements depend only on the position and type of actuators, specifically here on the position and width of the jets. The column is positioned in the matrix in a row which depends only on the position of the sensor. In this way the elements of $\boldsymbol{\xi}_k$ involved in m_k are only the nodes involved in the implementation of the boundary conditions on the jets. The only element of $\mathbf{W}_k$ involved in m_k is the horizontal velocity at the node on which the sensor is placed. In other words, the sensitivity map m_k is large if actuation involves large components of $\boldsymbol{\xi}_k$ and the sensor involves large components of $\mathbf{W}_k$. Obviously, the same result can be straightforwardly generalized to the case in which x_s, y_s, and θ_s vary with continuity in their definition range, as in the present case, so reaching to a well-known result, i.e., that actuation must be placed in regions where the adjoint mode $\boldsymbol{\xi}_k$ is large and sensors where the direct mode $\mathbf{W}_k$ is large for the control to be effective on mode σ_k.

The criterion that is followed here for the initial placement of the sensor in order to start an iterative procedure for the minimization of f is based on the maps m_k related to the N_a eigenvalues, which are monitored through the function f. Those eigenvalues are (i) the unstable eigenvalue (in our case this is the one with non-negative real part and we denote it as the first one, i.e., σ_1) and (ii) those eigenvalues that are dangerously affected by the control so that they can easily become unstable due to the effect of the feedback control. We will show in the following that those eigenvalues are well determined in the particular flow considered here and they are two (plus their complex-conjugate ones, which are not considered as explained above), leading thus to $N_a=3$. The initial position that is selected for the sensor must be a compromise between the following conditions:

(1) maximization of the displacement of the unstable eigenmode in the direction parallel to the real axis: $\delta\,\mathrm{Re}(\sigma_1)$;
(2) the sign of $\delta\,\mathrm{Re}(\sigma_k)$ for $k=2,\ldots,N_a$ must be the same as that of $\delta\,\mathrm{Re}(\sigma_1)$; this condition assures that, at least for very small values of the gain coefficient, if the unstable eigenvalue is moved toward the stable region of

the complex plane, also the potentially dangerous eigenvalues move in the same direction and, thus, they remain stable;

(3) the amplitude of $\delta \mathrm{Re}(\sigma_k)$ must be similar to that of $\delta \mathrm{Re}(\sigma_1)$; this condition avoids that the displacement of the potentially dangerous eigenvalues is much larger than that of the unstable one. Indeed, in this case, while the displacement of the unstable eigenvalue would remain in a linear limit for which estimation (10) is still accurate, this could not happen for some of the remaining eigenvalues which, thus, might become unstable although the condition specified above at point (2) is satisfied.

Conditions (2) and (3) are aimed at keeping under control the movement of the potentially dangerous eigenvalues. It is important to remark here that the three conditions listed above are followed only for the selection of the initial position of the sensors and they are meaningful only in the limit in which Eq. (17) remains accurate, i.e., for small values of the feedback coefficient. As the feedback coefficient increases to realistic values, the displacement of the eigenvalue is no longer given by Eq. (17) and the use of this equation would be misleading, as shown in the following. However, it is possible to reach a given value of the feedback gain by successive linearizations of the system, letting the position of the sensor to be changed at each step, obviously respecting possible constraints on its position; this is the spirit leading to the use of an iterative algorithm for the minimization of f in which the position of the sensor is a free parameter of the control design.

D. Schematic résumé of the design procedure

The main elements of the procedure are the following.

- A flow that is globally unstable.
- The steady unstable solution of the flow equations, which is the target of the control.
- A strategy for the feedback control of the flow; in our case a proportional feedback control, characterized by some design parameters. Here these are the position of the sensors (x_s, y_s) and, for each sensor, the component of the measured velocity (θ_s) and feedback coefficient (k_s).
- A global stability analysis of the direct and adjoint flow equations, linearized around the steady state.
- The identification of a set of N_a eigenvalues of the uncontrolled system that includes the unstable ones and those potentially destabilized by actuation.
- Definition of a function f, which depends on the position of the selected eigenvalues in the complex plane, such that, when this is minimized, the N_a eigenvalues are in the stable region of the complex plane.

Once the above elements are given, the algorithm is sketched in schematic form in Fig. 2.

V. ASSESSMENT OF THE CONTROL DESIGN ALGORITHM

A. Computational domain and discretization parameters

With reference to Fig. 1, the computational domain used in this paper is characterized by $L_{\mathrm{in}}=12.5L$ and $L_{\mathrm{out}}=20.5L$. This choice has been done on the basis of previous numerical simulations of the same flow (see, for instance, Weller *et al.*[13] and Buffoni *et al.*[29]). The dimensions of the actuators are the same as in Weller *et al.*,[13] i.e., the jets are centered around $x=0.3L$ and its total width is $0.16L$. These dimensions are reasonably comparable with those used in other works documented in the literature as, for instance, in Park *et al.*[4] and in Min and Choi.[9]

The strategy to design the control described above has been applied using a stretched Cartesian grid, GR1, made by 540 (N_x) and 330 (N_y) points in the x and the y direction, respectively, with a resulting resolution varying from $(\Delta x_{\min}=\Delta y_{\min}\simeq 1.1\times 10^{-2}L)$ on the body to $(\Delta x_{\max}\simeq 1.2\times 10^{-1}L,\ \Delta y_{\max}\simeq 6.9\times 10^{-2}L)$ at the outflow boundary. In this grid, 15 nodes are placed on the exit surface of each jet. The controls computed with GR1 have been systematically verified using a more refined grid to check grid convergence of the results. This grid, GR2, is characterized by $N_x=810$, $N_y=494$, $\Delta x_{\min}=\Delta y_{\min}\simeq 7.4\times 10^{-3}L$, $\Delta x_{\max}\simeq 8.1\times 10^{-2}L$, and $\Delta y_{\max}\simeq 4.6\times 10^{-2}L$, and 22 grid points are placed on the exit surface of each jet.

B. Spectrum of the linearized operator in the uncontrolled case

The spectrum of the uncontrolled system, linearized around Q_b, has been investigated for different values of Re before designing the controller. Moreover, preliminary tests have been carried out to identify the stable eigenvalues that are affected by the control and that are close to the unstable region of the complex plane, so that they can become unstable due to the control itself. As explained above, the position of such eigenvalues is included among the arguments of f. In the present case two complex stable eigenvalues have been identified as dangerously affected by the control (σ_2 and σ_3). Their position for different values of Re is plotted in Fig. 3, together with the unstable eigenvalue of the system (σ_1) (all of them are complex and we consider only those with positive imaginary parts). We recall here that the critical Reynolds number for the primary instability in the considered configuration is $\mathrm{Re}_{\mathrm{cr}}\simeq 59$ (see Camarri and Giannetti[24]).

In the examples of application of the control design strategy reported in the following, the first sensor is constrained to remain on the symmetry line $(y=0)$ and to measure only the y component of velocity, leaving thus two free parameters, i.e., the x position of the sensor and the associated feedback coefficient. For the initial placement of the sensor, the real parts of the maps $m_1(x_s,0,\pi/2)$, $m_2(x_s,0,\pi/2)$, and $m_3(x_s,0,\pi/2)$, associated, respectively, with the eigenvalues σ_1, σ_2, and σ_3 of the uncontrolled case (see Fig. 3), are plotted for different values of Re in Figs. 4(a)–4(c), respectively. Only the real parts are considered because, in the considered case, we are only interested to the

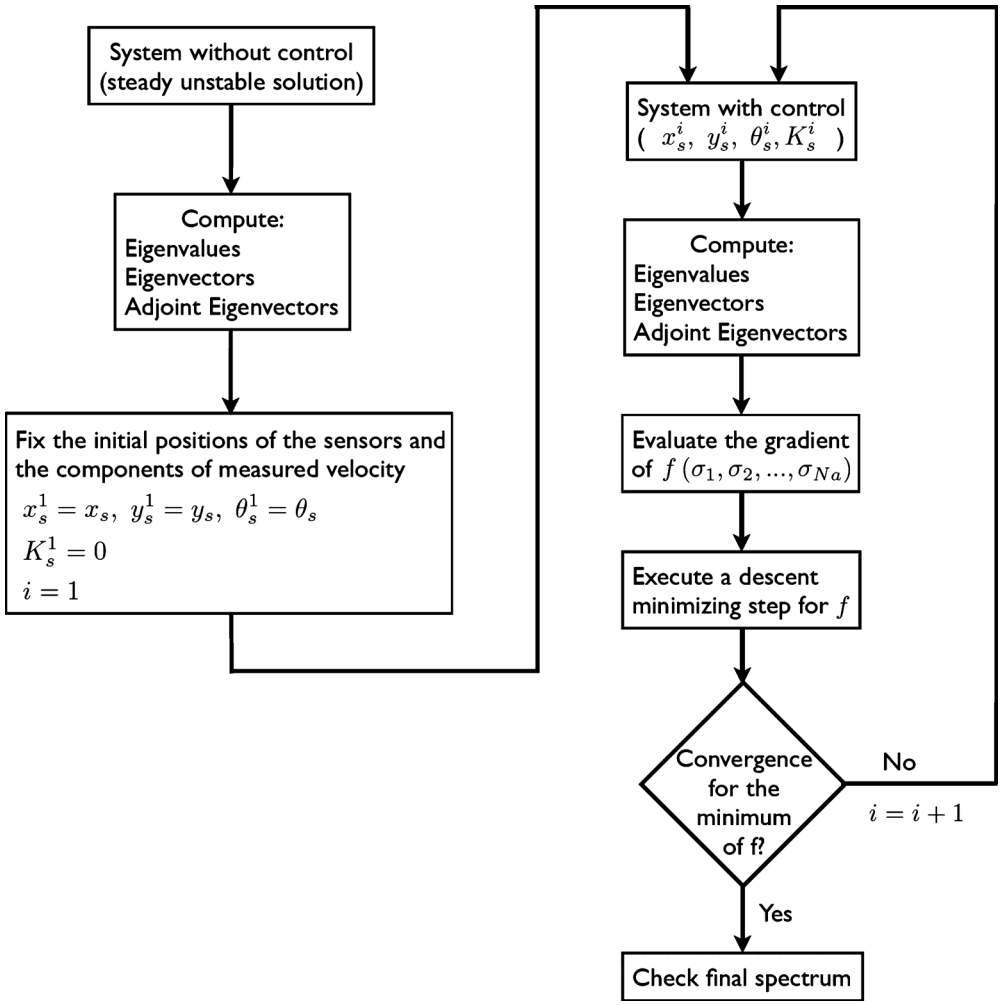

FIG. 2. Sketch of the strategy for the design of the control.

component of the eigenvalue displacement which is parallel to the real axis and, also, the function f depends only on the real part of the monitored eigenvalues. In Fig. 4(d) the three maps obtained at Re=120 using GR1 and GR2 are plotted together, showing grid convergence of the maps in the near wake.

For the sake of completeness, the real part of the maps $m_1(x_s, y_s, 0)$ and $m_1(x_s, y_s, \pi/2)$ obtained as a function of x_s and y_s using grid GR1 at Re=90 are also reported here in Fig. 5 [note that the map for Re=90 reported in Fig. 4(a) is a cut of Fig. 5(b) taken at section $y=0$]. In the same figures, a dotted line delimits the region in space where the real part of map m_1 is larger, in absolute value, than that of the remaining two maps, m_2 and m_3. This means that, if a sensor is placed with an infinitesimal feedback coefficient in that region, this causes a displacement of σ_1 parallel to the real axis of the complex plane which is larger than that caused for σ_2 and σ_3 [see condition (3) followed for the initial placement of the sensors described in Sec. IV C]. The maps in Figs. 4 and 5 highlight that the placement of the sensors too far from the cylinder largely increases the sensitivity to the control of the other stable modes, amplifying the "water-bed" effect and thus reducing the margin for the control of the unstable mode. This is in agreement with the experimental observations by Roussopoulos.[2]

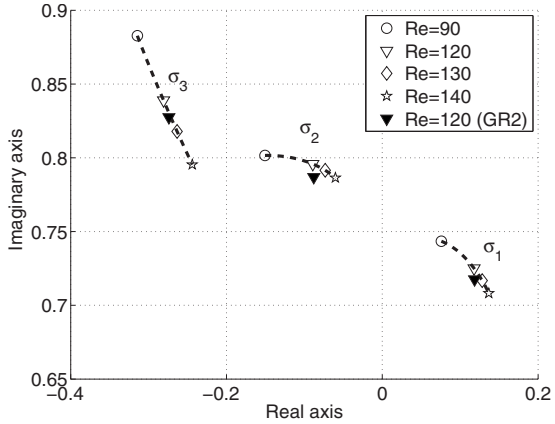

FIG. 3. Position, for different values of Re, of the three eigenvalues considered as the arguments of the function f, obtained on grid GR1 (empty symbols) and GR2 (full symbol).

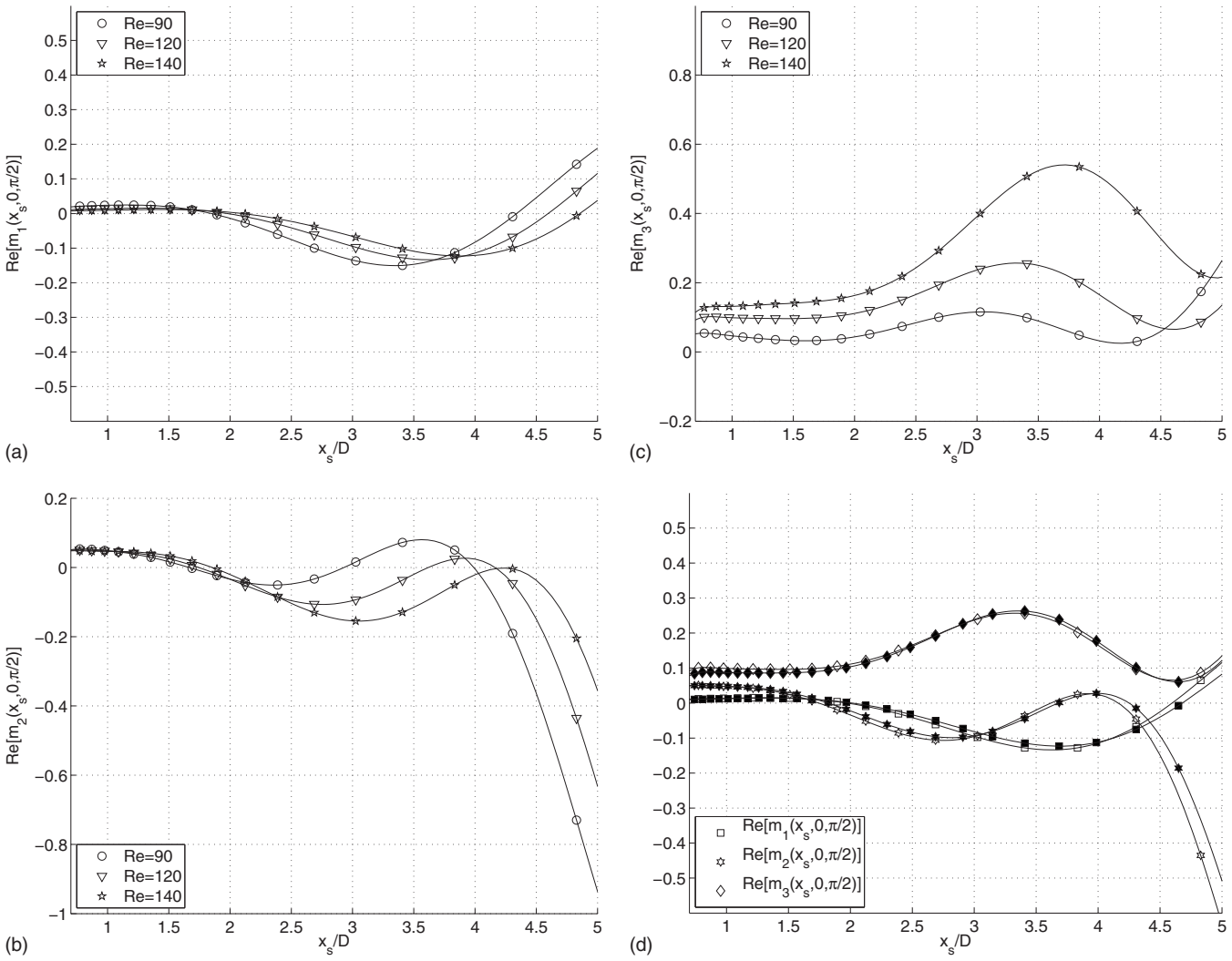

FIG. 4. Real parts of the maps $m_1(x_s,0,\pi/2)$ (a), $m_2(x_s,0,\pi/2)$ (b), and $m_3(x_s,0,\pi/2)$ (c) as a function of x_s and Re obtained using GR1; the three maps obtained using grids GR1 (empty symbols) and GR2 (full symbols) for Re=120 are reported together in (d).

C. Design of the control: Examples

As a first example, a control has been designed at Re=90, which is about 1.5 times larger than Re_{cr}. As explained above, a single-sensor has been introduced as a first step, which was constrained to remain on the symmetry line ($y=0$) and to measure only the y component of velocity ($\theta=\pi/2$). For the minimization of f as a function of x and K, two iterative methods have been indifferently used here. The first one is basically a gradient method with a limiter on the size of the step which is taken at each iteration. This limiter is important because the eigenvalues at each step are found using as initial localization their position at the previous step, and for this procedure to be effective, the displacement of the eigenvalues across each step needs to be sufficiently small. The other method used to minimize f is the MATLAB implementation of a subspace trust-region method, which is based on the interior-reflective Newton method described by Coleman and Li.[30] The initial values of x and K for the iterative algorithm were selected following the criterion described in Sec. IV C and using the maps in Fig. 4, which describe the sensitivity of the real parts of the three selected eigenvalues as a function of the x position of a sensor associated with an infinitesimal feedback. Consequently $K^{\mathrm{ini}}=0$, while we selected $x^{\mathrm{ini}}=2.5$; with this choice we have a ratio between m_1, m_2, and m_3 approximately equal to 1.00:0.63:-1.00 and $m_1<0$. This means that with the considered sensor and for infinitesimal positive values of K, σ_1 and σ_2 move toward the stable region of the complex plane while the opposite happens for σ_3, and the displacements along the imaginary axis of the complex plane are in a ratio which is equal to the ratios between m_1, m_2, and m_3. Thus, σ_1 moves more rapidly than σ_2 in the complex plane and, moreover, it is the eigenvalue closest than the others to the boundary of the stable region. Again, we recall that the previous statements are valid only for infinitesimal values of the feedback coefficient K. The target value r_t [see Eq. (15)] has been set equal to $r_t=-0.05$ which is a reasonable target if one considers the uncontrolled spectrum plotted in Fig. 3. The minimization procedure terminated correctly, leading to $x\simeq 3.01$ and $K\simeq 0.61$, and the final position of the three eigenvalues is plotted using empty circles in Fig. 6, showing that the system was stabilized (the spectrum of the operator was also

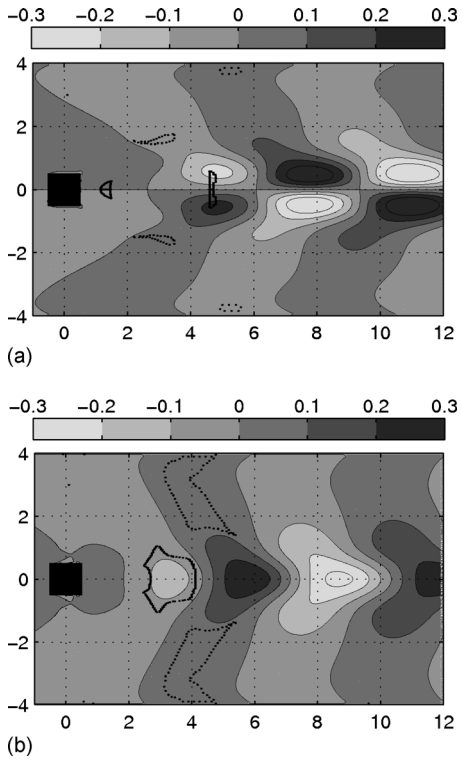

FIG. 5. Real parts of the maps $m_1(x_s, y_s, 0)$ (a) and $m_1(x_s, y_s, \pi/2)$ (b) as a function of x_s and y_s obtained using GR1 at Re=90.

checked *a posteriori*) and that the target r_t was successfully reached. In the figure cited above, a line connects the initial (cross) and the final position of each eigenvalue; that line is only for visualization purposes and it is the locus of the positions of the eigenvalue obtained by fixing $x=3.01$ and by progressively increasing K up to $K \simeq 0.61$. Note that, for small values of K, the directions in which the eigenvalues are displaced agree with the maps reported in Fig. 4. The spectrum of the controlled system has been checked also using grid GR2, in order to check its sensitivity to grid refinement, and the results are reported using filled circles in Fig. 6. The

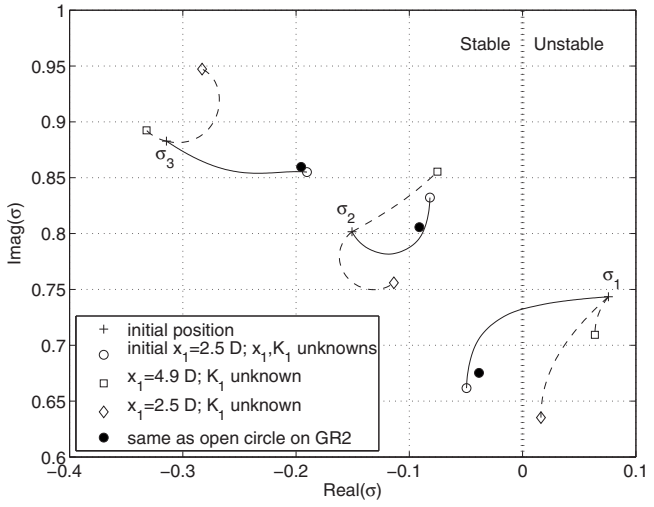

FIG. 6. Position of the monitored eigenvalues in the uncontrolled case and for three examples of control which are commented in the text (Re=90).

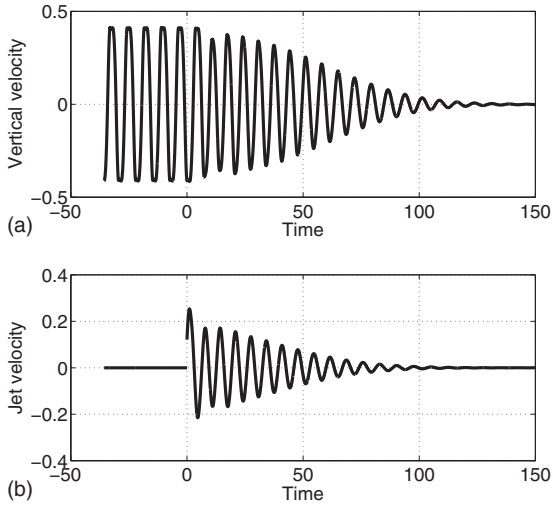

FIG. 7. Unsteady simulation (grid GR1) at Re=90, controller ($x=3.01$, $y=0$, and $K=0.61$) impulsively applied at $t=0$: (a) vertical velocity measured at point (5,0) and (b) normal velocity at the exit of the upper jet (positive values stand for outflowing jet).

linear stability limit of the controlled system has been evaluated using GR1 and it was found that the system becomes unstable for $108 < \mathrm{Re} < 109$. We recall that, in the uncontrolled case, $\mathrm{Re}_{cr} \simeq 59$. Moreover, the robustness of the designed controller has been tested in an unsteady nonlinear simulation (grid GR1, $\Delta t = 7.5 \times 10^{-3}$) by activating it impulsively once the vortex-shedding instability was nonlinearly saturated. As stated above, there is no guarantee that the controller is able to stabilize the flow in such conditions and this capability must be explored *a posteriori*. In the present case the controller was able to completely stabilize the flow, as shown in Fig. 7(a), where the vertical velocity measured at the point of coordinates (5,0) is plotted against time. In Fig. 7(b) we also plotted the time history of the velocity at the exit of the jets, which is proportional, through K, to the velocity measured by the sensor. In the two figures cited above, the origin of the time axis is chosen so that the controller is activated impulsively at time $t=0$.

As already stated above, the information provided by the maps reported in Fig. 4 is the result of a linearized analysis in K and is not sufficient, in general, to properly place the sensor of the controller. In order to prove this statement, we carried out two additional tests. In the first one, we constrained the sensor to remain in the position selected according to the maps, $x=2.5$, which was the initial position for the iterative minimization procedure of the previous test. Consequently, the only design parameter in the present case is the feedback coefficient K, whose initial value is again set to zero. At the end of the minimization procedure, we found $K=0.98$ but the system was not stabilized, as shown in Fig. 6, where the final position of the three eigenvalues is plotted with a diamond-shaped symbol. The trajectory of the eigenvalue σ_1 as K is progressively increased indicates that the minimization ended correctly, since the isolines of the function f_b are straight lines parallel to the imaginary axis and eigenvalues σ_2 and σ_3 in this case do not contribute to the value of f, their real part being smaller than r_t. In the second

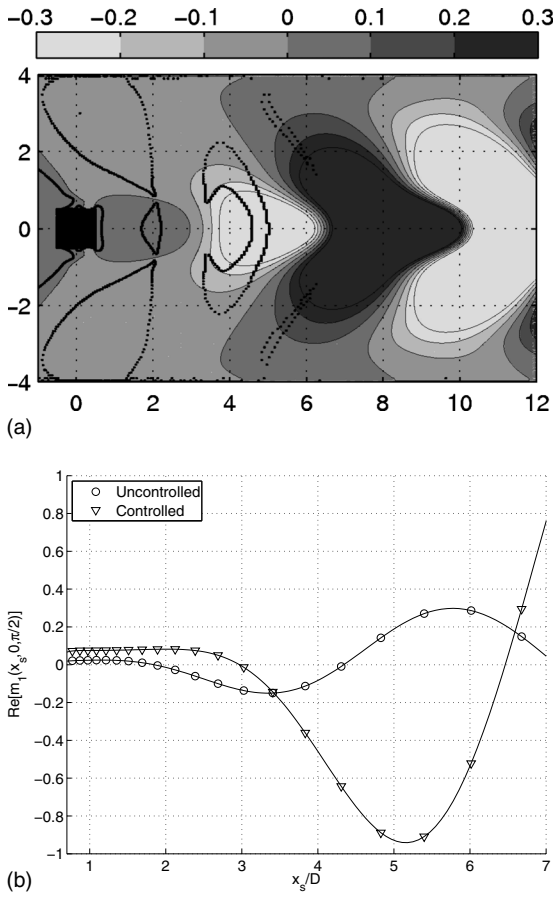

FIG. 8. (a) Real part of the map $m_1(x_s, y_s, \pi/2)$ obtained as a function of x_s and y_s using GR1 at Re=90 for the successfully controlled case; a section at $y_s=0$ is reported in (b), together with the corresponding map for the uncontrolled case.

test, the x position of the sensor was constrained, too, but with a different value: $x=4.9$. At this position the map m_1 is twice as large as that measured at $x=2.5$, and the ratio between the three maps is approximately equal to $1:-5:1.3$, with $m_1>0$. As in the previous case, at the end of the minimization procedure $K\simeq -0.13$ and the system was not stabilized, as shown by the final positions of the eigenvalues, plotted in Fig. 6 using square symbols. Moreover, the unstable eigenvalue is more distant from the stability region than that obtained positioning the sensor at $x=2.5$, although its sensitivity to the feedback control is higher in this second case. The previously described tests clearly show that the information contained in the maps of Fig. 4 cannot be extrapolated for the values of K which are typically required in the present control problem. In particular, when the system is controlled with a certain value of K, the maps m_i, and consequently the controlled modes and their adjoint ones, change in such a way that the position of the sensor that was effective when the uncontrolled system was considered, turns out to be progressively inadequate to stabilize the system. Conversely, if the x coordinate of the sensor is also left free and optimized together with K, the sensor is moved in proper positions as the feedback coefficient K is iteratively changed, according to a local linearization of the controlled system.

As an example, we have reported in Fig. 8(a) the real part of the map $m_1(x_s, y_s, \pi/2)$ at the end of the successful control design, i.e., when the sensor of vertical velocity is placed at $x\simeq 3.01$ with a feedback coefficient $K\simeq 0.61$. The comparison with the corresponding map for the uncontrolled flow, Fig. 5(b), clearly put in evidence marked differences and confirms what affirmed above concerning the validity of the initial linearized analysis on the uncontrolled system. For a more quantitative comparison, we have reported together in Fig. 8(b) the maps $m_1(x_s, 0, \pi/2)$ obtained for the uncontrolled and controlled cases. The curve for the uncontrolled case is the same one reported in Fig. 4(a) for Re=90 and that has been used for the initial placement of the sensor for the iterative design of the control. Note that the real part of map m_1 on the final position of the sensor $(m_1(3.01, 0, \pi/2))$, at the end of the control design, has a negligible value; this is correct as the eigenvalues σ_2 and σ_3 do not affect the value of f in that case.

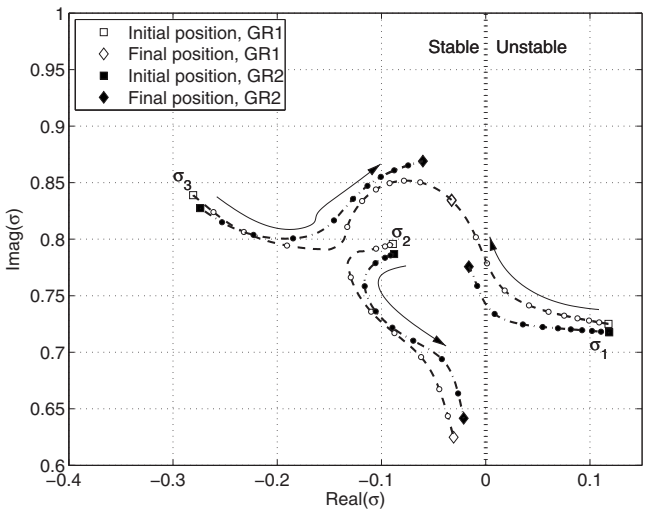

FIG. 9. Position of the monitored eigenvalues in the uncontrolled case and in the controlled case with one sensor at Re=120.

In the present case, the design of the control strategy becomes progressively more difficult as Re is increased, as it is well-known[1] and also clear from Fig. 3. For this reason, in order to test the proposed procedure in more challenging flow conditions, we repeated the first test described above at Re=120. In particular, a single-sensor is used, which is located on the symmetry line $y=0$ and which measures the y component of velocity. In agreement with the maps reported in Fig. 4, the initial values $K^{\text{ini}}=0$ and $x^{\text{ini}}=3.1$ have been selected for the iterative optimization of the x position of the sensor and of the associated feedback coefficient K. Also in this case the optimization procedure ended successfully leading to $x\simeq 3.41$ and $K\simeq 0.66$, and the initial and final positions of the three monitored eigenvalues are reported in Fig. 9. Again, the dotted lines are plotted only for simplifying the identification of the final positions of the eigenvalues; they have been obtained fixing $x=3.41$ and progressively increasing K from 0 to its final value; the small circles on the dotted lines indicate the position of the eigenvalues assumed at equispaced intervals in K. The sensitivity of the eigenvalue positions to the grid refinement in the controlled case is expected to be larger than in the uncontrolled case, especially

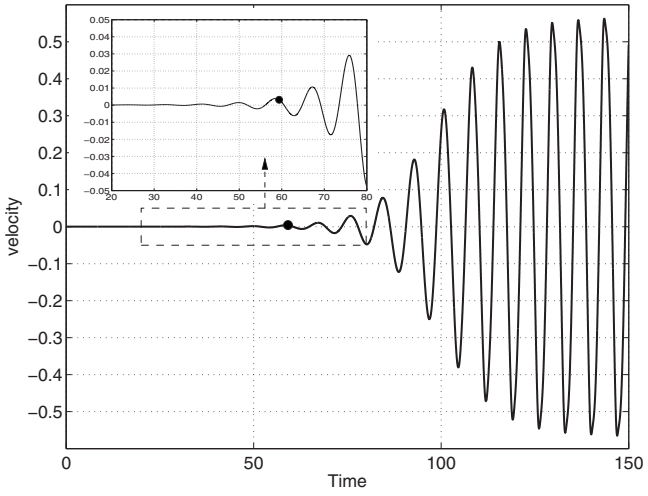

FIG. 10. Vertical velocity measured at the position (3,0) in the unsteady simulation of the transient flow obtained at Re=120 starting the simulation from the unstable steady solution of the flow equations; the filled point indicates the limit in time after which the control, when activated impulsively, is not able to stabilize the flow.

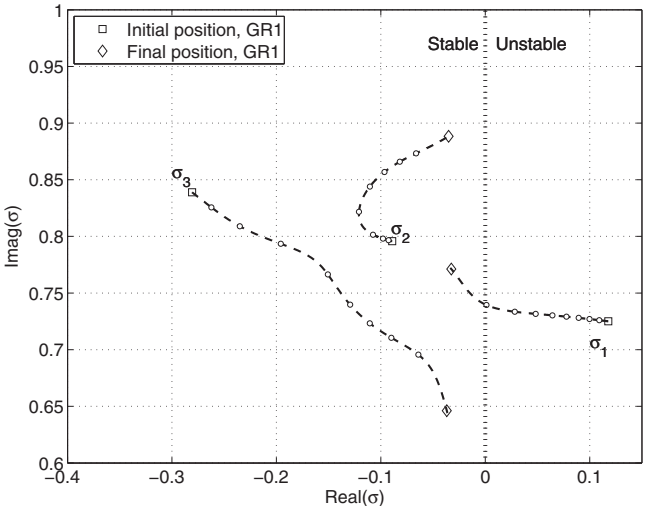

FIG. 11. Position of the monitored eigenvalues in the uncontrolled case and in the controlled case with two sensors at Re=120.

as the Reynolds number is increased. Also, the assumption that the velocity profile at the jet exit is constant is expected to increase this sensitivity with respect to a smooth velocity profile on the same jet. This is confirmed by comparing Fig. 3 with Fig. 9. Note that the grid sensitivity that is carried out here is particularly severe since we obtained GR2 by a refinement which is concentrated in the near the cylinder, and, although both the grids used are definitely fine, the number of nodes lying on one jet boundary varies significantly when passing from grid GR1 (15 nodes) to GR2 (22 nodes). However, this aspect does not interfere with the capability of the tests documented here to prove the effectiveness of the proposed control strategy. Indeed, we recall that the strategy is not formulated here using a continuous formulation and discretized successively, but it is directly applied to the discretized system. In this sense, the representativeness of the discretized system with respect to the original continuous problem is separated by the design of the controller. The robustness of the resulting controller has been also tested in a time-dependent simulation. Compared with the case at Re=90, here the controller does not stabilize the flow if it is activated once the vortex-shedding instability is saturated. However, an idea of the robustness of the controller has been obtained by activating the controller at different times after the impulsive start of the flow and by locating the time limit after which the controlled flow is unstable. This point has been reported in Fig. 10, together with the vertical velocity measured at the position (3,0) in the uncontrolled case. The figure shows that the control is not robust and it is effective when the disturbance amplitude is about 120 times smaller than the saturated level. As already pointed out, the properties of the controller in the nonlinear regime cannot be explored using the linearized analysis on which the design of the controller itself is based. However, in case it would be possible, for particular systems, to relate a given configuration of the eigenvalues to desired properties of the controlled system, that configuration might be approached by minimizing a suitable function analogous to that in Eq. (15).

The use of more sensors or more degrees of freedom for each sensor is supposed to increase the possibility of the controller to minimize the function f. An example is given here by using two sensors of vertical velocity placed on the symmetry line $y=0$ at Re=120. The initial feedback coefficients are zero and the initial positions are $x_1^{\text{ini}}=3.1$ (as in the previous case with only one sensor) and $x_2^{\text{ini}}=2.1$. The minimization converged to the final positions $x_1 \simeq 3.33$ and $x_2 \simeq 2.11$ and the final feedback coefficients $K_1 \simeq 0.67$ and $K_2 \simeq -0.10$. In this case, the final position of the monitored eigenvalues in the controlled system is different with respect to that obtained in the previous test using only one sensor, as shown in Fig. 11. The figure shows that the final positions of the eigenvalues σ_1 and σ_3 are well separated, in contrast with the case with one sensor. However, there is no any substantial gain in terms of the stability margin which is obtainable by the control. Indeed, the imposed target $r_t=-0.05$ is not reached by σ_1 since the other eigenvalues σ_2 and σ_3 also approach the penalized region of the complex plane and, at the end of the controller design, they are moving toward the unstable region of the complex plane. Consequently, as the three eigenvalues are treated here in the same way [see Eq. (15)], the procedure stops when the three eigenvalues approximately have the same real part, which is smaller than r_t. This happens both when one or two sensors are used, as shown in Figs. 9 and 11, respectively. The reduced margin of gain in stability observed here as the number of sensors is increased has been confirmed by a series of tests carried out on the maximum Reynolds number at which the controller is able to stabilize the flow. Those tests, not reported here for the sakes of brevity, show that there is not a substantial gain in using more degrees of freedom related to the sensors. In our opinion, this behavior is probably related to the limited controlling capabilities of the adopted actuation, which involves only one degree of freedom. This assumption might be thus verified by enriching the degrees of freedom of the

actuation. However, this aspect has not been further explored here since it does not limit the validity of the proposed strategy of control design.

VI. CONCLUSIONS

In the present work a simple proportional feedback control is designed to suppress the vortex-shedding instability in the wake of a prototype bluff-body flow. This objective is a pretext to propose a general strategy for designing a controller, a strategy which is independent of the type of actuation and sensors. The idea is to exploit the sensitivity analysis of the primary instability of the wake and of other appropriate modes, with respect to the design parameters of the controller. In particular, the sensitivity analysis provides a linearized prediction of the displacement of some selected eigenvalues in the complex plane as a function of the controller parameters. However, especially at Reynolds numbers well above the critical one for the primary instability of the wake, the final values of the design parameters are such that the initial sensitivity analysis, carried out on the uncontrolled flow, is no longer valid. In this connection, it is shown in this paper that the information provided by the initial sensitivity analysis alone is not sufficient to design a controller which stabilizes the flow. Therefore, the design is done iteratively by successive linearizations carried out during the design process. This general strategy is applied here to design a proportional feedback control. Apart from possible constraints, the position of the sensors, the direction along which velocity is measured, and the feedback coefficients are outputs of the design procedure.

In the particular flow considered here, actuation is provided by two out-of-phase localized jets on the cylinder surface, and velocity sensors are employed. It is shown in this paper that the proposed strategy, with actuation which is fixed *a priori* by analogy with other works documented in the literature, leads to a successful control up to a Reynolds number which is at least twice as large as the critical one for primary instability, using only one velocity sensor.

Note, however, that the control is designed on the basis of the linearized system dynamics; thus, the characteristics of the controller, when this is applied sufficiently far from the design state so that the nonlinearities start to play a significant role, must be explored *a posteriori*. This is an important feature of the control, since it determines the capability of the controller to stabilize the flow even if this is activated when the vortex-shedding instability has already started. It has been shown here that this basin of attraction becomes progressively smaller as the flow Reynolds number is increased. Indeed, while at $\mathrm{Re}=90$, the controller is able to stabilize the flow even if it is activated when the vortex-shedding instability is nonlinearly saturated, at $\mathrm{Re}=120$ the robustness of the control in this sense definitely becomes weaker. Lastly, we point out that the control design proposed here needs a global stability analysis of the discretized linearized flow equations and of its adjoint system. Considering the number of degrees of freedom involved, this imply high computational costs which, although affordable in two-dimensional problems, might become extremely cpu-demanding in three-dimensional cases. However, due to the number of degrees of freedom involved in the discrete flow model, a real pole-placement approach would be definitely unfeasible even in 2D cases.

In concluding, we would like to stress that the same ideas proposed here can be extended to different control strategies, including passive controls, and that the sensitivity analysis of the global instability is the key element for the proposed approach. In this regard, a passive control could be designed by building an additional small body in the flow, and the design of this body could be carried out iteratively, using at each iteration the same sensitivity analysis documented by Marquet *et al.*[23] The design could, for instance, be carried out by successive linearizations also starting from the nonlinearly saturated instability, using a Floquet analysis and the ideas proposed by Luchini *et al.*[31]

ACKNOWLEDGMENTS

The authors are grateful to Professor P. Luchini and to Dr. F. Giannetti for having provided a part of the computational tools used in the present work and for the useful discussions. The simulations documented here have been carried out thanks to the computational resources of IMB (Bordeaux).

[1] H. Choi, W. Jeon, and J. Kim, "Control of flow over a bluff body," Annu. Rev. Fluid Mech. **40**, 113 (2008).
[2] K. Roussopoulos, "Feedback control of vortex shedding at low Reynolds numbers," J. Fluid Mech. **248**, 267 (1993).
[3] X. Huang, "Feedback control of vortex shedding from a circular cylinder," Exp. Fluids **20**, 218 (1996).
[4] D. S. Park, D. M. Ladd, and E. W. Hendricks, "Feedback control of von Kármán vortex shedding behind a circular cylinder at low Reynolds numbers," Phys. Fluids **6**, 2390 (1994).
[5] M.-M. Zhang, L. Cheng, and Y. Zhou, "Closed-loop-controlled vortex shedding and vibration of a flexibly supported square cylinder under different schemes," Phys. Fluids **16**, 1439 (2004).
[6] J.-P. Raymond, "Boundary feedback stabilization of the two dimensional Navier–Stokes equations," SIAM J. Control Optim. **45**, 790 (2006).
[7] J.-W. He, R. Glowinski, R. Metcalfe, A. Nordlander, and J. Periaux, "Active control and drag optimization for flow past a circular cylinder: I. Oscillatory cylinder rotation," J. Comput. Phys. **163**, 83 (2000).
[8] B. Protas and A. Styczek, "Optimal rotary control of the cylinder wake in the laminar regime," Phys. Fluids **14**, 2073 (2002).
[9] C. Min and H. Choi, "Suboptimal feedback control of vortex shedding at low Reynolds numbers," J. Fluid Mech. **401**, 123 (1999).
[10] W. R. Graham, J. Peraire, and K. Y. Tang, "Optimal control of vortex shedding using low-order models. Part II: Model-based control," Int. J. Numer. Methods Eng. **44**, 973 (1999).
[11] M. Bergmann, L. Cordier, and J.-P. Brancher, "Optimal rotary control of the cylinder wake using proper orthogonal decomposition reduced-order model," Phys. Fluids **17**, 097101 (2005).
[12] S. Siegel, K. Cohen, and T. McLaughlin, "Numerical simulations of a feedback controlled circular cylinder wake," AIAA J. **44**, 1266 (2006).
[13] J. Weller, S. Camarri, and A. Iollo, "Feedback control by low-order modelling of the laminar flow past a bluff body," J. Fluid Mech. **634**, 405 (2009).
[14] F. Li and N. Aubry, "Feedback control of a flow past a cylinder via transverse motion," Phys. Fluids **15**, 2163 (2003).
[15] B. Protas, "Linear feedback stabilization of laminar vortex shedding based on a point vortex model," Phys. Fluids **16**, 4473 (2004).
[16] M. Pastoor, L. Henning, B. R. Noack, R. King, and G. Tadmor, "Feedback shear layer control for bluff body drag reduction," J. Fluid Mech. **608**, 161 (2008).
[17] P. Mokhasi and D. Rempfer, "Optimized sensor placement for urban flow measurement," Phys. Fluids **16**, 1758 (2004).
[18] K. Cohen, S. Siegel, and T. McLaughlin, "A heuristic approach to effec-

tive sensor placement for modeling of a cylinder wake," Comput. Fluids **35**, 103 (2006).
[19]K. Willcox, "Unsteady flow sensing and estimation via the gappy proper orthogonal decomposition," Comput. Fluids **35**, 208 (2006).
[20]M. Buffoni, S. Camarri, A. Iollo, E. Lombardi, and M. V. Salvetti, "A non-linear observer for unsteady three-dimensional flows," J. Comput. Phys. **227**, 2626 (2008).
[21]C. Antoniades and P. D. Christofides, "Integrating nonlinear output feedback control and optimal actuator/sensor placement for transport-reaction processes," Chem. Eng. Sci. **56**, 4517 (2001).
[22]F. Giannetti and P. Luchini, "Structural sensitivity of the cylinder first instability of the cylinder wake," J. Fluid Mech. **581**, 167 (2007).
[23]O. Marquet, D. Sipp, and L. Jacquin, "Sensitivity analysis and passive control of cylinder flow," J. Fluid Mech. **615**, 221 (2008).
[24]S. Camarri and F. Giannetti, "On the inversion of the Kármán street in the wake of a confined square cylinder," J. Fluid Mech. **574**, 169 (2007).
[25]S. Turki, H. Abbassi, and S. B. Nasrallah, "Effect of the blockage ratio on the flow in a channel with built-in square cylinder," Comput. Mech. **33**, 22 (2003).
[26]M. Breuer, J. Bernsdorf, T. Zeiser, and F. Durst, "Accurate computations of the laminar flow past a square cylinder based on two different methods: Lattice-Boltzmann and finite-volume," Int. J. Heat Fluid Flow **21**, 186 (2000).
[27]T. A. Davis, "Algorithm 832: UMFPACK—an unsymmetric-pattern multifrontal method," ACM Trans. Math. Softw. **30**, 196 (2004).
[28]V. Hernandez, J. E. Roman, and V. Vidal, "SLEPc: A scalable and flexible toolkit for the solution of eigenvalue problems," ACM Trans. Math. Softw. **31**, 351 (2005).
[29]M. Buffoni, S. Camarri, A. Iollo, and M. V. Salvetti, "Low-dimensional modelling of a confined three-dimensional wake flow," J. Fluid Mech. **569**, 141 (2006).
[30]T. F. Coleman and Y. Li, "An interior, trust region approach for nonlinear minimization subject to bounds," SIAM J. Optim. **6**, 418 (1996).
[31]P. Luchini, F. Giannetti, and J. O. Pralits, "Structural sensitivity of linear and nonlinear global modes," in *Proceedings of the Fifth AIAA Theoretical Fluid Mechanics Conference*, Seattle, Washington, 23–26 June 2008 (Curran Associates, Red Hook, NY, 2008), AIAA Paper No. 2008-4227.